zjv01916/zjv1962d16z | xppws | S=1 | 7/22/16 | 20:27 | 4/C Fig: 5,6,7 | ArtID: 01106-16 | NLM: research-article | CE: KFH

Editor: Caughey | Section: Prions | Designation: T

AMERICAN SOCIETY FOR MICROBIOLOGY | Journal of Virology

Guinea Pig Prion Protein Supports Rapid Propagation of Bovine Spongiform Encephalopathy and Variant Creutzfeldt-Jakob Disease Prions

AQ: au Joel C. Watts,[a,c*] Kurt Giles,[a,c] Daniel J. Saltzberg,[b] Brittany N. Dugger,[a,c] Smita Patel,[a] Abby Oehler,[a] Sumita Bhardwaj,[a] Andrej Sali,[b,e,f] Stanley B. Prusiner[a,c,d]

AQ: aff Institute for Neurodegenerative Diseases,[a] California Institute for Quantitative Biosciences (QB3),[b] and Departments of Neurology,[c] Biochemistry and Biophysics,[d] Bioengineering and Therapeutic Sciences,[e] and Pharmaceutical Chemistry, University of California, San Francisco, San Francisco, California, USA[f]

ABSTRACT

The properties of bovine spongiform encephalopathy (BSE) and variant Creutzfeldt-Jakob disease (vCJD) prions are faithfully maintained upon transmission to guinea pigs. However, primary and secondary transmissions of BSE and vCJD in guinea pigs result in long incubation periods of ~450 and ~350 days, respectively. To determine if the incubation periods of BSE and vCJD prions could be shortened, we generated transgenic (Tg) mice expressing guinea pig prion protein (GPPrP). Inoculation of Tg(GPPrP) mice with BSE and vCJD prions resulted in mean incubation periods of 210 and 199 days, respectively, which shortened to 137 and 122 days upon serial transmission. In contrast, three different isolates of sporadic CJD prions failed to transmit disease to Tg(GPPrP mice). Many of the strain-specified biochemical and neuropathological properties of BSE and vCJD prions, including the presence of type 2 protease-resistant PrP^{Sc}, were preserved upon propagation in Tg(GPPrP) mice. Structural modeling revealed that two residues near the N-terminal region of α-helix 1 in GPPrP might mediate its susceptibility to BSE and vCJD prions. Our results demonstrate that expression of GPPrP in Tg mice supports the rapid propagation of BSE and vCJD prions and suggest that Tg(GPPrP) mice may serve as a useful paradigm for bioassaying these prion isolates.

IMPORTANCE

Variant Creutzfeldt-Jakob disease (vCJD) and bovine spongiform encephalopathy (BSE) prions are two of the prion strains most relevant to human health. However, propagating these strains in mice expressing human or bovine prion protein has been difficult because of prolonged incubation periods or inefficient transmission. Here, we show that transgenic mice expressing guinea pig prion protein are fully susceptible to vCJD and BSE prions but not to sporadic CJD prions. Our results suggest that the guinea pig prion protein is a better, more rapid substrate than either bovine or human prion protein for propagating BSE and vCJD prions.

Prions are self-propagating, β-sheet-rich protein aggregates that play a central role in many human neurodegenerative diseases (1, 2). Disorders such as Creutzfeldt-Jakob disease (CJD) in humans, chronic wasting disease in deer and elk, scrapie in sheep, and bovine spongiform encephalopathy (BSE) are caused by the accumulation of prions composed of an alternatively folded and infectious conformer of the prion protein (PrP) in the brain (3, 4). Prion diseases can also be zoonotic, as in the case of variant CJD (vCJD), which is caused by the consumption of BSE-contaminated beef products (5, 6). The cellular form of PrP, PrP^{C}, is a host-encoded, glycophosphatidylinositol (GPI)-anchored neuronal glycoprotein composed of a flexibly disordered N-terminal domain and a predominantly α-helical C-terminal domain (7–9). During disease, PrP^{C} undergoes a profound conformational change into an aggregation-prone, misfolded conformer termed PrP^{Sc}, which is enriched in β-sheet content (10). The most commonly encountered forms of PrP^{Sc} are partially resistant to degradation by proteases such as proteinase K (PK), which allows differentiation of PrP^{C} and PrP^{Sc} (11).

Different strains of PrP^{Sc} have been described and can be classified according to the clinical manifestation of disease, the observed patterns of cerebral PrP^{Sc} deposition, the molecular properties of PrP^{Sc}, and the incubation periods upon inoculation into laboratory animals (12–15). The strain-specified properties of PrP^{Sc} are enciphered within the conformation of the protein aggregates (16, 17). The transmission of prions from one species to another is usually limited by the so-called "species barrier" (18). Generally, disease transmission is efficient when PrP^{Sc} and PrP^{C} are from the same species (19), whereas species mismatches can result in prolonged incubation periods on primary passage, as well as strain adaptation (20). However, there are several exceptions to this rule, including in the bank vole (BV), which expresses a PrP that can efficiently replicate prions from many different species (21–25). In contrast to the species barrier, which reflects differences between PrP^{Sc} and PrP^{C} amino acid sequences, strain barriers are dictated by the conformation of PrP^{Sc}. For instance, vCJD

Received 7 June 2016 Accepted 14 July 2016

Accepted manuscript posted online ●●●

Citation Watts JC, Giles K, Saltzberg DJ, Dugger BN, Patel S, Oehler A, Bhardwaj S, Sali A, Prusiner SB. 2016. Guinea pig prion protein supports rapid propagation of bovine spongiform encephalopathy and variant Creutzfeldt-Jakob disease prions. J Virol 90:000–000. doi:10.1128/JVI.01106-16.

Editor: B. Caughey, Rocky Mountain Laboratories

Address correspondence to Stanley B. Prusiner, stanley.prusiner@ucsf.edu.

* Present address: Joel C. Watts, Tanz Centre for Research in Neurodegenerative Diseases and Department of Biochemistry, University of Toronto, Toronto, Ontario, Canada.

prions are not transmitted well to transgenic (Tg) mice expressing human PrP (HuPrP) despite the identical amino acid sequences of PrP^{C} and PrP^{Sc} (26). In contrast, vCJD and BSE prions efficiently transmit disease to wild-type (WT) mice (26–31), although there are many differences in the amino acid sequences between the recipient mouse and the infecting bovine PrP (BoPrP) or HuPrP. The species and strain barriers are often collectively referred to as "transmission barriers" for prion replication, for which a given PrP^{C} can only replicate a subset of PrP^{Sc} conformations (32, 33).

Human CJD prions have been successfully transmitted to both primates (34) and guinea pigs (*Cavia porcellus*) (35–38). Efficient transmission of BSE (39, 40) and vCJD (39) prions to guinea pigs has also been reported. The biochemical and neuropathological hallmarks of BSE and vCJD prions were faithfully maintained upon propagation in guinea pigs, suggesting that these animals may be useful for studying these isolates. However, the incubation periods for BSE and vCJD prions upon primary passage in guinea pigs were very long (~450 and ~350 days, respectively) (39), reducing the attractiveness of using guinea pigs for prion bioassays. Furthermore, it is unknown whether the permissiveness of guinea pigs for BSE and vCJD prions is encoded within the sequence of guinea pig PrP (GPPrP) or is due to a distinct feature of guinea pig neurophysiology.

We hypothesized that Tg mice that overexpress GPPrP would, like guinea pigs, be susceptible to BSE and vCJD prions and exhibit abbreviated incubation periods when challenged with these isolates. Therefore, we generated Tg(GPPrP) mice and then inoculated them with BSE, vCJD, and sporadic CJD (sCJD) prions. All inoculated Tg(GPPrP) mice were susceptible to BSE and vCJD prions, and the incubation periods were approximately half of those of guinea pigs, revealing that expression of GPPrP in Tg mice enables relatively rapid propagation of these isolates. These data argue that Tg(GPPrP) mice may be an excellent model for bioassaying BSE and vCJD prions.

MATERIALS AND METHODS

Ethics statement. Mouse husbandry and bioassays were carried out in accordance with the recommendations of the Guide for the Care and Use of Laboratory Animals (Institute of Laboratory Animal Resources, National Academies Press, Washington, DC). All animal protocols were approved by the University of California, San Francisco (UCSF), Institutional Animal Care and Use Committee (breeding colony and production of Tg rats and mice [AN084871] and incubation periods of prion and other neurodegenerative diseases [AN084950]). All BSE and vCJD transmission experiments were performed under biosafety level 3 conditions.

Generation of Tg mice. The GPPrP open reading frame was PCR amplified from guinea pig genomic DNA (Zyagen) with the following primers: 5′-CTATATGGATCCACCATGGCAAATGCCGGCTGCTGG CTGC-3′ (forward) and 5′-CTATATTCTAGATCATCCCACTATCAG GAAGATCAGG-3′ (reverse). The amplified DNA was digested with BamHI and XbaI and then inserted into plasmid pcDNA3 to create plasmid pcDNA3.GPPrP. Following DNA sequence verification, the guinea pig coding sequence was PCR amplified from pcDNA3.GPPrP with flanking SalI restriction sites with the following primers: 5′-CTATATGTCGA CACCATGGCAAATGCCGGCTGC-3′ (forward) and 5′-CTATATGTC GACTCATCCCACTATCAGGAAGAT-3′ (reverse). The PCR product was then digested with SalI and ligated into a SalI-digested and dephosphorylated cos.Tet cosmid vector (41), which drives the expression of proteins in the brain by using the Syrian hamster PrP promoter. The transgene cassette was then excised by digestion with NotI, purified by agarose gel electrophoresis, and then microinjected into the pronuclei of fertilized eggs obtained from FVB-$Prnp^{0/0}$ mice. Potential founder animals were identified by Southern blotting with a DNA probe specific for the 3′ untranslated region of Syrian hamster *Prnp* and then backcrossed to FVB-$Prnp^{0/0}$ mice (42) to confirm germ line transmission of the transgene. Three lines of Tg(GPPrP) mice were obtained: Tg23441, Tg23447, and Tg23454.

Prion isolates. The following prion isolates were used in this study: a human vCJD isolate obtained from a patient brain sample generously provided by Robert Will and James Ironside of the National CJD Surveillance Unit (United Kingdom); BSE prions from the brain of a naturally infected cow (isolate PG31/90) that were passaged four times in Tg mice expressing BoPrP (43); human prions from sCJD patients exhibiting the MM1, MM2, or VV2 disease subtype; and the mouse-passaged scrapie strain RML, which was maintained in WT CD-1 mice. The guinea pig-passaged vCJD isolate was generated by pooling brain homogenates from three clinically ill, vCJD-inoculated guinea pigs, whereas the guinea pig-passaged BSE isolate was created by pooling brain homogenates from four clinically ill, BSE-inoculated guinea pigs (39). The guinea pig-passaged sCJD sample was generated by pooling the brain homogenates from three clinically ill guinea pigs that had been inoculated with a guinea pig-passaged sCJD isolate (39), which was kindly provided by Jun Tateishi of Kyushu University in Japan.

Mouse bioassays. Brain homogenates (10% [wt/vol] in calcium- and magnesium-free phosphate-buffered saline [PBS]) were generated with a Precellys 24 bead beater and then diluted to a final concentration of 1% (wt/vol) in 5% (wt/vol) bovine serum albumin. Weanling (~8-week-old) Tg23454 mice were anesthetized with isoflurane and then intracerebrally inoculated in the right parietal lobe with 30 μl of diluted brain homogenate with a 27-gauge syringe. The inoculated mice were monitored daily for routine health assessment and checked three times weekly for the development of clinical signs of neurological illness by using the standard diagnostic criteria for assessing prion disease in mice (44). Mice were euthanized when two or more signs of disease were apparent, and their brains were removed and either fixed in 10% neutral buffered formalin for neuropathological analysis or snap-frozen on dry ice and then stored at −80°C for biochemical studies.

Enzymatic digestions of proteins. Ten percent (wt/vol) brain homogenates in PBS were generated with a Precellys 24 homogenizer. Samples were treated with 100 μg/ml PK for 1 h at 37°C, and then digestions were stopped by adding phenylmethylsulfonyl fluoride to a final concentration of 2 mM, followed by an equal volume of 2× lithium dodecyl sulfate loading buffer. Samples were boiled for 10 min prior to immunoblot analysis. Peptide-*N*-glycosidase F (PNGase F) digestions were performed according to the manufacturer's protocol (New England BioLabs).

Immunoblotting. Samples were loaded onto 10% NuPAGE gels (Life Technologies) and then subjected to electrophoresis with the 2-(*N*-morpholino)ethanesulfonic acid buffer system. Proteins were transferred to polyvinylidene difluoride membranes, which were then blocked with blocking buffer (5% [wt/vol] nonfat milk in Tris-buffered saline containing 0.05% [vol/vol] Tween 20 [TBST]) for 1 to 2 h at room temperature. The membranes were then incubated with horseradish peroxidase-conjugated anti-PrP antibody HuM-P (45) for 1 to 2 h at room temperature. Following three washes with TBST, the membranes were developed with an enhanced chemiluminescence detection system (GE Healthcare) and then exposed to X-ray film. AQ: A AQ: B

Quantification of transgene expression levels. Protein concentrations in brain homogenates from WT FVB or Tg(GPPrP) mice were determined with the bicinchoninic acid assay (Thermo Scientific). Normalized samples were prepared in 1× NuPAGE loading buffer containing β-mercaptoethanol, boiled for 5 min, and then analyzed by immunoblotting as described above. For the Tg(GPPrP) samples, serial dilutions relative to WT FVB mouse brains were made in 1× NuPAGE loading buffer. Relative levels of GPPrP were compared to those of WT MoPrP in FVB mice and expressed as *n*-fold differences.

Neuropathology. Formalin-fixed brains were embedded in paraffin, and then brain sections (8 μm thick) were cut and mounted onto slides.

For each brain, coronal sections were analyzed at four different levels: the striatum, the hippocampus/thalamus, the midbrain, and the cerebellum. Sections were either processed for immunohistochemistry (IHC) or stained directly with hematoxylin and eosin (H&E) to assess vacuolation. For IHC, endogenous tissue peroxidases were first inhibited by incubation in 3% hydrogen peroxide solution (prepared in methanol) for 30 min. Sections were then subjected to hydrolytic autoclaving at 121°C in citrate buffer for 10 min in order to expose protein epitopes. After cooling, slides were blocked with 10% (vol/vol) normal goat serum for 1 h at room temperature and then incubated with anti-PrP mouse monoclonal antibody 3F4 (46) at a dilution of 1:1,000 overnight at 4°C. PrP deposits were visualized with the Vectastain ABC peroxidase kit (Vector Laboratories) and 3-3′-diaminobenzidine. Slides were counterstained with hematoxylin, and photographs were taken with the Axio Imager.A1 microscope (Carl Zeiss). Semiquantitative scoring of spongiform degeneration and PrP^{Sc} deposition in the brains of prion-inoculated mice was performed by assigning scores to different brain regions as follows: 0, no vacuolation/PrP^{Sc} deposition; 1, mild vacuolation/PrP^{Sc} deposition; 2, moderate vacuolation/PrP^{Sc} deposition; 3, severe vacuolation/PrP^{Sc} deposition. An individual blind to the experimental design conducted all of the neuropathological analyses.

Generation and analysis of PrP^{Sc} structural models. MoPrP, BoPrP, and GPPrP sequence alignments were constructed with Clustal Omega (47). One hundred structural models of each PrP sequence were produced with the automodel class in MODELLER (48) for each of the β-helix (49) and parallel in-register β-sheet (PIRIBS) (50) PrP^{Sc} models, as well as for monomeric $MoPrP^{C}$ (PDB code 1AG2) and $BoPrP^{C}$ (PDB code 1DWZ). Identification of hydrogen bonds was performed by using previously reported geometric constraints (51) and implemented with Tcl scripts in visual molecular dynamics (VMD) (52). Void volumes in the PIRIBS-A models were calculated and visualized with CAVER Analyst 1.0 (53) by utilizing a 0.5-Å sphere radius. All other model visualization and figure preparation was performed with VMD.

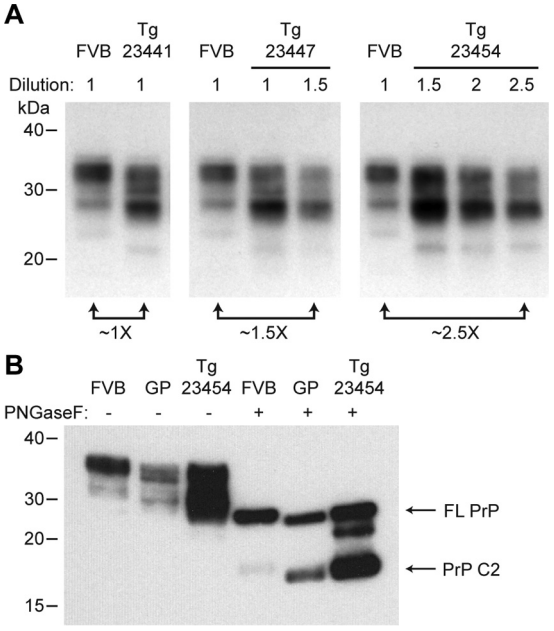

FIG 1 Expression of GPPrP in Tg mice. (A) Immunoblot analyses of PrP levels in brain homogenates from three different lines of Tg(GPPrP) mice compared to those of WT FVB mice. Dilutions were made relative to FVB brain homogenate. GPPrP expression levels with respect to the level of PrP found in WT mice: Tg23441 mice, ~1×; Tg23447 mice, ~1.5×; Tg23454 mice, ~2.5×. (B) Immunoblot analysis of PrP species in brain homogenates from WT FVB mice, guinea pigs (GP), and Tg23454 mice with (+) or without (–) PNGase F digestion. Following digestion, both full-length (FL) PrP and the C2 fragment are apparent. In both panels, PrP was detected with the antibody HuM-P. Molecular masses of migrated protein standard markers are shown in kilodaltons to the left of each panel.

RESULTS

GPPrP is polymorphic at codon 62 (which corresponds to codon 71 in mouse PrP [MoPrP] and codon 72 in HuPrP), where either a glycine or a serine residue can be present (39, 54). The coding sequence for GPPrP with serine at residue 62 was inserted into the cos.Tet vector, which has been widely used to drive the expression of PrP and other transgenes in the brain (41). Following microinjection into zygotes isolated from PrP knockout mice, we obtained three lines of Tg(GPPrP) mice by germ line transmission, which were designated Tg23441, Tg23447, and Tg23454. Semiquantitative immunoblotting revealed that Tg23441 mice express GPPrP at levels approximately equivalent to those of MoPrP in WT mice, whereas the Tg23447 and Tg23454 lines overexpressed GPPrP at approximately 1.5- and 2.5-fold, respectively, the levels in WT mice (Fig. 1A). Since PrP levels appeared to be slightly lower in guinea pigs than in WT mice (Fig. 1B), we estimate that Tg23454 mice overexpress GPPrP at approximately 3-fold the level found in guinea pigs.

A portion of PrP^{C} in the brain normally undergoes endoproteolytic processing to produce C-terminal cleavage fragments, referred to as C1 and C2 (55). In all three lines of Tg(GPPrP) mice, the predominant PrP species that we observed in the brain by immunoblotting was not the diglycosylated full-length species, which was the most abundant PrP species in WT FVB mice (Fig. 1A). After removal of the N-linked oligosaccharides from PrP, bands corresponding to full-length and C2 species were apparent (Fig. 1B). The epitope for the HuM-P antibody used to detect MoPrP and GPPrP encompasses residues 96 to 105 (MoPrP numbering) (45) and therefore does not detect the PrP C1 fragment. The relative proportions of the PrP C2 fragment were increased following removal of the N-linked sugars in Tg23454 mice and in guinea pigs (Fig. 1B), indicating that the predominant PrP band corresponds to the PrP C2 cleavage fragment. Following deglycosylation, full-length GPPrP migrated slightly faster than MoPrP because the sequence of GPPrP differs from that of other mammalian PrPs in that it lacks 10 residues N terminal to the octapeptide repeats in the flexible N-terminal region of the protein (Fig. 2) (39). Interestingly, the PrP C2 fragment in guinea pigs and Tg23454 mice also migrated more rapidly than the mouse C2 fragment, despite the fact that the C2 cleavage site occurs on the C-terminal side of the 10-residue deletion in GPPrP (Fig. 1B). One possible explanation is that C2 cleavage occurs on the basis of the length of the PrP N-terminal domain instead of in a sequence-specific manner, as has been observed for PrP C1 cleavage (56).

No signs of spontaneous neurological dysfunction were observed in any of the Tg(GPPrP) lines up to 600 days of age (Table 1). We did not conduct extensive neuropathological analysis or perform serial transmission experiments to test for the presence of subclinical prion disease. To examine the susceptibility of these Tg lines to prions, we inoculated them with sCJD prions that had been previously passaged twice in guinea pigs (39). This guinea pig-passaged sCJD isolate was originally derived from an sCJD patient with an unknown disease subtype (37) and was last passaged in guinea pigs that express GPPrP with glycine at codon 62. All three lines of Tg(GPPrP) mice developed prion disease following inoculation with this strain of guinea pig-passaged sCJD pri-

FIG 2 Alignment of GPPrP, BoPrP, and MoPrP sequences. Positions where GPPrP and BoPrP contain the same residue that differs from the corresponding residue in MoPrP are shaded in gray. The two positions interrogated further (residues 142 and 144 in the MoPrP sequence) are also outlined in black. Sequence alignment was performed with Clustal Omega 1.2.1.

ons, with mean incubation periods ranging from 136 to 157 days (Table 1), which was ~100 days shorter than the incubation period of guinea pig-passaged sCJD prions in guinea pigs (39). Interestingly, there did not appear to be a correlation between the GPPrP expression level in the Tg mice and the resultant incubation period of guinea pig-passaged sCJD prions (Fig. 3A).

We used the Tg23454 line for the remainder of our transmission studies because these mice expressed the highest levels of GPPrP and exhibited the shortest mean incubation period following inoculation with guinea pig-passaged sCJD prions. Intracerebral inoculation of Tg23454 mice with BSE prions resulted in efficient disease transmission, with a mean incubation period of 210 days, which was ~230 days shorter than the corresponding incubation period in guinea pigs (Table 2). For these studies, we used BSE prions that had previously been passaged in Tg(BoPrP) mice since the incubation periods of bovine- and Tg(BoPrP)-derived BSE prions in Tg(BoPrP) mice were essentially identical (33). BSE prions passaged in guinea pigs (39) and Tg23454 mice were injected into Tg23454 mice for serial passaging, and the resulting mean incubation times (~140 days) were similar (Fig. 3B). Inoculation of Tg23454 mice with brain homogenate from a vCJD patient resulted in a mean incubation period of 199 days, which was ~170 days shorter than the incubation period of vCJD prions in guinea pigs (Table 2). Secondary passage of vCJD prions in Tg23454 mice reduced the mean incubation period to 122 days, which was shorter than the mean incubation period (~150 days) of guinea pig-passaged vCJD prions injected into Tg23454 mice (Fig. 3C). One possible explanation for this discrepancy between incubation periods is that the guinea pig-passaged vCJD sample was isolated from a guinea pig with glycine at codon 62 of PrP (39), whereas Tg23454 mice express GPPrP with serine at residue 62. These results demonstrate that both BSE and vCJD prions can be efficiently propagated in Tg(GPPrP) mice.

None of the Tg23454 mice that were inoculated with brain homogenate from sCJD patients exhibiting the MM1, MM2, or VV2 disease subtype developed clinical signs of prion disease, suggesting that expression of GPPrP creates a substantial transmission barrier for these strains (Table 3) and consistent with the low disease transmission rates observed upon inoculation of guinea pigs with prions from CJD patients (37, 57). The three sCJD isolates inoculated into Tg23454 mice are distinct from the sCJD isolate originally used to generate the guinea pig-passaged sCJD prions (37). No signs of disease were observed in Tg23454 mice inoculated with the RML strain of mouse-passaged scrapie prions. Like the Tg23454 mice, guinea pigs were also resistant to infection with RML prions (39). Since we did not perform neuropatholog-

TABLE 1 Transmission of guinea pig-passaged sCJD prions to Tg(GPPrP) mice

Line	PrP expression level (n-fold)[a]	Uninoculated: Mean age (days) at spontaneous disease occurrence	Uninoculated: n/n_0[b]	Inoculated with guinea pig-passaged sCJD prions: Mean incubation period (days) ± SEM	Inoculated with guinea pig-passaged sCJD prions: n/n_0
Tg23441	1.0	>603	0/7	143 ± 3	6/6
Tg23447	1.5	>603	0/5	157 ± 2	8/8
Tg23454	2.5	>606	0/7	136 ± 2	7/7

[a] PrP expression levels were determined relative to the expression of mouse PrP in FVB mice.
[b] n, number of ill mice; n_0, number of mice under observation.

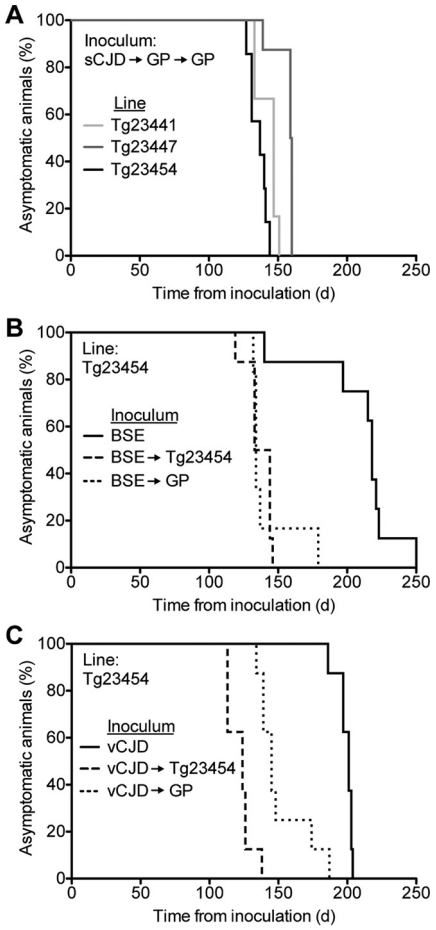

FIG 3 Transmission of prions to Tg(GPPrP) mice. (A) Kaplan-Meier survival curves of Tg23441 mice (light gray line, $n = 6$), Tg23447 mice (dark gray line, $n = 8$), and Tg23454 mice (black line, $n = 7$) inoculated with an isolate of guinea pig-passaged sCJD prions. (B) Kaplan-Meier survival curves of Tg23454 mice inoculated with BSE prions (solid line, $n = 8$), BSE prions passaged once in Tg23454 mice (dashed line, $n = 8$), or BSE prions passaged once in guinea pigs (dotted line, $n = 6$). (C) Kaplan-Meier survival curves of Tg23454 mice inoculated with vCJD prions (solid line, $n = 8$), vCJD prions passaged once in Tg23454 mice (dashed line, $n = 8$), or vCJD prions passaged once in guinea pigs (dotted line, $n = 8$). d, days.

ical analysis or passaging experiments with Tg23454 mice inoculated with sCJD or RML prions, we cannot exclude the presence of subclinical prion disease in these animals.

The brains of Tg23454 mice that were inoculated with BSE or vCJD prions exhibited PK-resistant PrP (Fig. 4A). No PK-resistant PrP was observed in the brain of an uninoculated Tg23454 mouse at 606 days of age, consistent with the absence of clinical signs of spontaneous neurological illness in these animals (Table 1). Distinct strains of prions can be distinguished by the electrophoretic mobility of the unglycosylated PK-resistant PrP fragment on an immunoblot. Type 1 strains migrate to ~21 kDa, whereas type 2 strains migrate to ~19 kDa (15). Both BSE and vCJD are classified as type 2 prion strains, and upon primary and secondary propagations in Tg23454 mice, a type 2 PrP^{Sc} signature was observed in the brain (Fig. 4B). Inoculation of Tg23454 mice with guinea pig-passaged vCJD and BSE prions also produced type 2 PrP^{Sc} (Fig. 4B). Sporadic CJD prions that have been passaged in guinea pigs exhibit type 1 PrP^{Sc} (39), and type 1 PrP^{Sc} was found in the brains of Tg23454 mice that had been inoculated with these prions (Fig. 4B). These results indicate that for BSE and vCJD prions, the strain type was preserved upon propagation in Tg23454 mice, arguing for the maintenance of prion strain fidelity.

A subset of the brains of BSE- and vCJD-inoculated Tg23454 mice was analyzed neuropathologically. Moderate-to-severe spongiform degeneration and PrP^{Sc} deposition were observed in all of the brain regions analyzed, with the exception of the cerebellum (Fig. 5A and B). BSE- and vCJD-challenged Tg23454 mice exhibited similar patterns of vacuolation and cerebral PrP^{Sc} deposition, supporting the assertion that BSE and vCJD are caused by the same prion strain (27, 58). Upon the first passage of BSE prions in Tg23454 mice, prominent loss of CA2 and CA3 neurons was apparent in the hippocampus (Fig. 5C). In vCJD-inoculated Tg23454 mice, extensive cell loss was observed in all areas of the hippocampus, including the dentate gyrus (Fig. 5D). Abundant vacuolation was observed in the cerebral cortex in both BSE- and vCJD-inoculated mice (Fig. 5E and G) and was accompanied by large, coarse PrP^{Sc} deposits (Fig. 5F and H). Large clusters of vacuoles, as well as numerous coarse PrP^{Sc} deposits, were found in the hippocampus in Tg23454 mice upon secondary passage of the

TABLE 3 Attempts to transmit sCJD and RML prions to Tg23454 mice

Inoculum	Mean incubation period (days) ± SEM	n/n_0[a]
sCJD MM1	>525	0/8
sCJD MM2	>503	0/8
sCJD VV2	>481	0/6
RML	>503	0/8

[a] n, number of ill mice; n_0, number of mice under observation.

AQ: D

TABLE 2 Transmission of BSE and vCJD prions to Tg23454 mice

	Primary transmission			Serial transmission		
Inoculum	Host	Mean incubation period (days) ± SEM	n/n_0	Host	Mean incubation period (days) ± SEM	n/n_0
BSE	Guinea pig	436 ± 28[b]	4/4	Guinea pig	310 ± 4[b]	6/6
				Tg23454	142 ± 8	6/6
	Tg23454	210 ± 11	8/8	Tg23454	137 ± 3	8/8
vCJD	Guinea pig	367 ± 4[b]	4/4	Guinea pig	287 ± 4[b]	5/5
	Tg23454	199 ± 2	8/8	Tg23454	122 ± 3	8/8

[a] n, number of ill mice; n_0, number of mice under observation.
[b] Previously published (39).

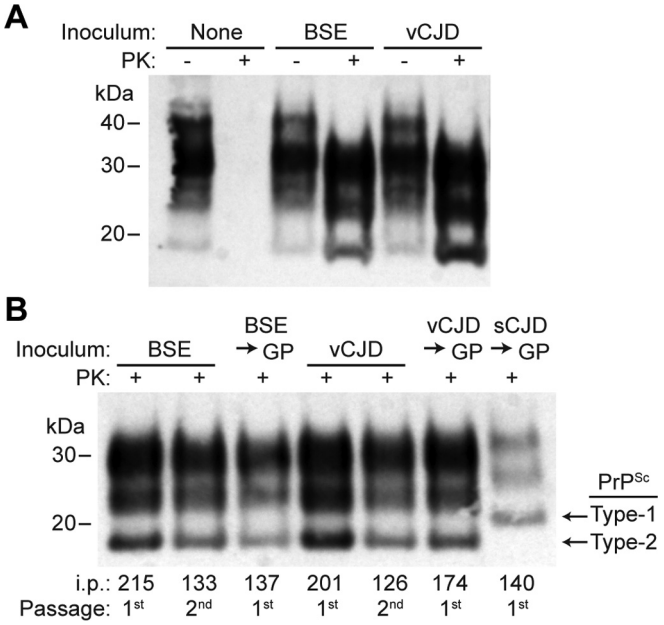

FIG 4 Biochemical typing of PrP^{Sc} in prion-inoculated Tg(GPPrP) mice. (A) Immunoblot analysis of PrP in brain homogenates from an uninoculated, asymptomatic Tg23454 mouse at 606 days of age (none); a clinically ill, BSE-inoculated Tg23454 mouse at 215 days postinoculation (BSE); and a clinically ill, vCJD-inoculated Tg23454 mouse at 201 days postinoculation (vCJD). Brain homogenates were either digested with PK (+) or left undigested (–). PK-resistant PrP^{Sc} was only observed in the mice inoculated with prions. (B) Immunoblot analysis of PK-resistant PrP^{Sc} in brain homogenates from Tg23454 mice inoculated with the prion isolates indicated. The brains of Tg23454 mice inoculated with BSE prions (first or second passage), guinea pig-passaged BSE prions, vCJD prions (first or second passage), or guinea pig-passaged vCJD prions exhibited type 2 PrP^{Sc}. In contrast, Tg23454 mice inoculated with guinea pig-passaged sCJD prions exhibited type 1 PrP^{Sc}. The incubation period (i.p.) of the mouse from which the brain was taken for immunoblotting is shown below each lane. In both panels, PrP was detected with the antibody HuM-P. Molecular masses of migrated protein standard markers are shown in kilodaltons to the left of each panel.

vCJD and BSE isolates (Fig. 5I to L). "Florid" PrP^{Sc} plaques, which are found in the brains of vCJD patients (5), were not observed in the brains of vCJD-inoculated Tg23454 mice. Overall, the neuropathological changes found in the brains of BSE- and vCJD-inoculated Tg23454 mice were similar to those observed in the brains of guinea pigs challenged with the same prion isolates (39).

That GPPrP supports the rapid, faithful propagation of BSE and vCJD prions but not RML prions suggests that sequence differences between MoPrP and GPPrP are responsible for the strain-specific propagation. We therefore searched for potential sequence features of GPPrP that could mediate these differential transmissions by comparing the amino acid sequences of GPPrP, BoPrP, and MoPrP. An alignment of these sequences revealed eight positions that were conserved between the GPPrP and BoPrP sequences but differed in the MoPrP sequence (Fig. 2). Three of these residues (residues 10, 14, and 17, numbered according to the sequence of MoPrP) are located within the N-terminal signal sequence of PrP and were not considered further. Similarly, residue 231, which occurs at or close to the GPI anchor attachment site, was not investigated because it does not appear in any structural models of PrP^{C} or PrP^{Sc}. At residues 108 and 137, either methionine or leucine residues are present in the three PrP sequences. However, these conservative amino acid changes are unlikely to lead to any major structural effects. Thus, we focused our analysis on residues 142 (serine in GPPrP and BoPrP, asparagine in MoPrP) and 144 (tyrosine in GPPrP and BoPrP, tryptophan in MoPrP), both of which are located near the N-terminal region of α-helix 1 in PrP^{C}. We assessed the impact of these variant residues on the structures of PrP^{C} by generating comparative models of the GPPrP, BoPrP, and MoPrP sequences by using as templates the nuclear magnetic resonance (NMR) structures of $MoPrP^{C}$ (PDB code 2L1H) and $BoPrP^{C}$ (PDB code 1DWZ). Although the structure of PrP^{Sc} is not known, we also generated models of the three PrP sequences by using four of the prevailing structural models of $MoPrP^{Sc}$: the left-handed β-helix model (49) and three PIRIBS models (50). AQ: C

Models based on PrP^{C} structures revealed that residues 142 and 144 are both solvent exposed (Fig. 6). Only small structural differences were observed among the models when the three sequences were threaded onto the $MoPrP^{C}$ and $BoPrP^{C}$ templates, suggesting that the residue 142 and 144 sequence variants would be predicted to have only a minor influence on the structure of PrP^{C}. Comparative models built from the $MoPrP^{Sc}$ scaffolds, however, suggested that the GPPrP and BoPrP variants at these two residues are incompatible with these $MoPrP^{Sc}$ models. In the β-helix model, residue 142 lies at the radial interface between trimers (Fig. 7A and C), while residue 144 is positioned at the interface between stacked monomers (Fig. 7B). In the β-helix model, the asparagine side chain of residue 142 in MoPrP participates in a hydrogen bond with the peptide backbone of the adjacent subunit with 78% occupancy. This interaction is observed less frequently in the models generated by using the BoPrP and GPPrP sequences (17 and 8%, respectively), which contain the shorter serine side chain that is less capable of bridging the intermolecular gap to form this interaction (Fig. 7C). All PIRIBS-based PrP^{Sc} models place residues 142 and 144 on a critical β-hairpin loop (residues 127 to 161) that participates in intermolecular interactions among stacked monomers (Fig. 7D and E). In particular, the tyrosine present at residue 144 in GPPrP and BoPrP structurally alters this loop in the PIRIBS-A model, with the side chain oriented outside the hairpin, resulting in a large, unfavorable channel penetrating the structure (Fig. 7F). Notwithstanding the limitations of predictions based on structural models, the above findings offer a plausible basis for why the GPPrP sequence cannot adopt the RML strain structure, as it would cause an unstable void in the framework. Since GPPrP and BoPrP sequences have similar discrepancies threading onto $MoPrP^{Sc}$ models, it is possible that a BSE strain structure is more consistent with the GPPrP sequence. F6 F7

DISCUSSION

In the studies reported here, we have determined that prions from BSE-afflicted cattle and vCJD patients transmit prion disease with 100% efficiency to Tg mice that express GPPrP, with incubation periods of ~200 days, which is about half the time needed to bioassay these strains in guinea pigs. Our results strongly suggest that the heightened susceptibility of guinea pigs to BSE and vCJD prions is mediated by the sequence of GPPrP. It should be noted that the vCJD and BSE bioassays were performed with guinea pigs that express GPPrP with glycine at codon 62, whereas the Tg(GPPrP) mice used for bioassays express GPPrP with serine at codon 62. Therefore, we cannot exclude the possibility that this polymorphism also influences the replication kinetics of vCJD

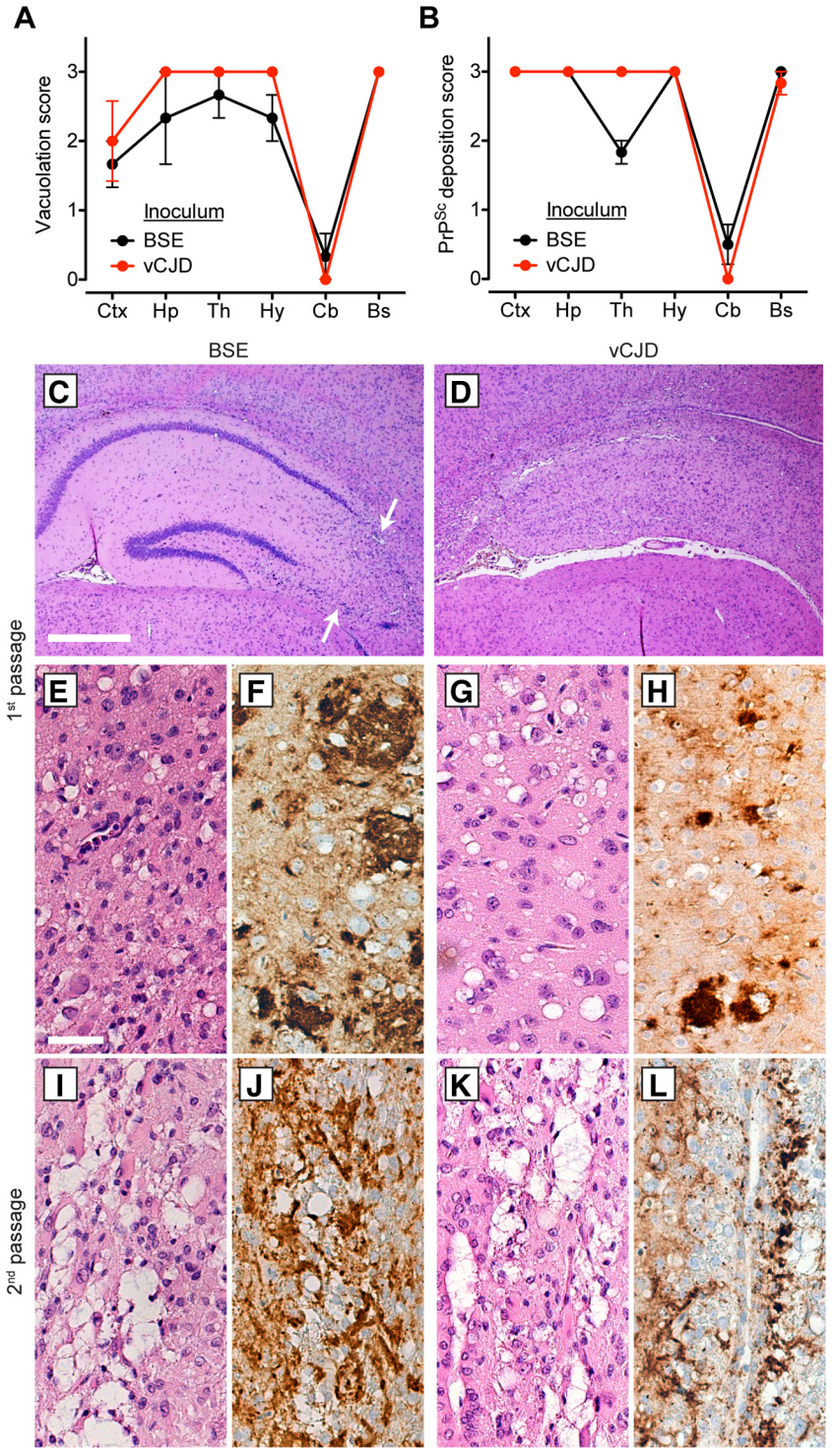

FIG 5 Neuropathological characterization of prion-inoculated Tg(GPPrP) mice. Semiquantitative vacuolation (A) and PrP^{Sc} deposition (B) scoring within the indicated brain regions from BSE (black, $n = 3$)- or vCJD (red, $n = 2$ or 3)-inoculated Tg23454 mice (first passage). Ctx, cortex; Hp, hippocampus; Th, thalamus; Hy, hypothalamus; Cb, cerebellum; Bs, brain stem. (C, D) Neuronal loss in the hippocampus of Tg23454 mice inoculated with BSE (C) or vCJD (D) prions (first passage), as visualized by H&E staining. The arrows in panel C denote loss of CA2 and CA3 neurons. The scale bar in panel C represents 500 μm and also applies to panel D. Vacuolation (E, G, I, K) and PrP^{Sc} deposition (F, H, J, L) in the brain following first or second passage of BSE (E, F, I, J) or vCJD (G, H, K, L) prions in Tg23454 mice. Vacuolation was visualized by H&E staining, and PrP^{Sc} deposition was assessed by immunohistochemistry with the antibody 3F4. For first-passage samples, the cerebral cortex is shown; for second-passage samples, the stratum oriens region of the hippocampus is displayed. The scale bar in panel E represents 50 μm and also applies to panels F to L.

COLOR

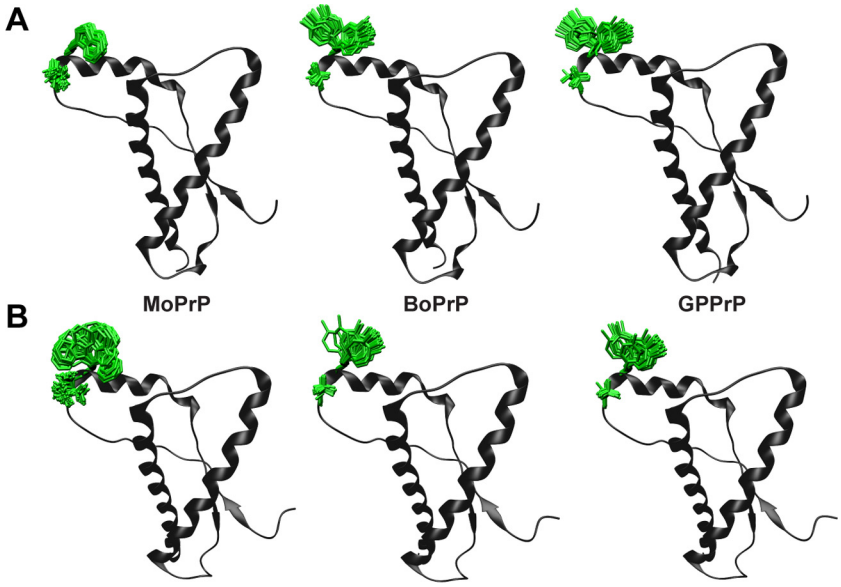

COLOR

FIG 6 Comparison of PrP^{C} structural models generated with MoPrP, BoPrP, or GPPrP sequences. (A) Models of MoPrP (left), BoPrP (center), and GPPrP (right) constructed by using the $MoPrP^{C}$ NMR structure (PDB code 2L1H). (B) Models of MoPrP (left), BoPrP (center), and GPPrP (right) constructed by using the $BoPrP^{C}$ NMR structure (PDB code 1DWZ). Stick representations show the positions of the residue 142 and 144 side chains (green; MoPrP numbering) for all 100 generated models.

and BSE prions. Furthermore, because BSE and vCJD prions are also transmitted efficiently, but slowly, to non-Tg mice (27, 30), other mouse-specific factors, such as putative prion replication cofactors (59, 60), may also play a role.

Tg(GPPrP) mice offer several advantages over guinea pigs for prion bioassays. In addition to the shorter disease incubation periods, mice are easier and cheaper to maintain, and they can be crossed with other Tg lines to permit monitoring of prion replication kinetics by bioluminescence imaging (61), for instance. However, the larger size of guinea pigs may provide unique bioassay benefits in some situations, such as when cerebrospinal fluid or blood sampling is required, or in imaging studies where an increased brain size may reveal additional levels of detail.

Studies of prion strains have been facilitated by the production of Tg mice expressing PrP genes from different species (62). Generally, incubation periods are shortened in the Tg mice because of the overexpression of PrP. While BSE prions present in either BSE-infected cattle or Tg(BoPrP) mouse brains can be efficiently transmitted to Tg mice expressing BoPrP (33, 43, 45, 58, 63), the incubation periods are long (~250 days), despite the overexpression of BoPrP. The incubation periods are also long upon the secondary passage of BSE prions in these mice (58). In contrast, the incubation period for BSE prions in Tg(GPPrP) mice, which overexpress PrP at lower levels than the aforementioned Tg mice expressing BoPrP (~2.5-fold versus ~8-fold), was only ~210 days upon primary passage and ~135 days upon secondary passage. This ~75-day decrease in the incubation period upon serial passage suggests that there is a transmission barrier for BSE prions in Tg(GPPrP) mice. However, it should be noted that 100% of the BSE-inoculated Tg(GPPrP) mice developed clinical prion disease, and we observed no evidence of BSE strain adaptation upon serial passage, either by neuropathological analysis of infected brain tissue or by PrP^{Sc} typing. Thus, the somewhat extended incubation period of BSE prions upon primary passage in Tg(GPPrP) mice is likely to result from slower prion replication kinetics, possibly because of the sequence mismatch between $BoPrP^{Sc}$ and $GPPrP^{C}$, or a difference in the prion titer between the BSE isolate and the Tg(GPPrP)-passaged BSE sample.

Variant CJD prions are transmitted efficiently to Tg mice expressing BoPrP, with incubation periods similar to those observed for BSE prions (~270 days) (33, 58), as well as to WT mice, with incubation periods of around 370 days (27). Curiously, the transmission of vCJD prions to Tg mice expressing sequence-matched HuPrP is remarkably inefficient, with only a few mice exhibiting clinical signs of disease following incubation periods of >600 days (26). On the basis of the aforementioned results, the propagation of vCJD prions was next studied in Tg mice expressing chimeric Hu/MoPrP molecules. In Tg22372 mice, which express chimeric PrP containing seven HuPrP-specific residues, the mean incubation periods for vCJD prions were 279 to 368 days (64). Shorter but highly variable incubation periods of vCJD prions (176 to 326 days) were observed in Tg1014 mice, which express chimeric PrP containing six HuPrP-specific residues (65). However, in both Tg22372 and Tg1014 vCJD-inoculated mice, a mixture of prion strains was apparent, indicative of strain selection or adaptation. In Tg(GPPrP) mice, the incubation period of vCJD prions was ~200 days on primary passage and ~120 days on secondary passage, and no strain adaptation was apparent by neuropathological and biochemical analyses. It should be noted that the vCJD prion isolates used in the aforementioned studies were not always the same, which complicates accurate comparisons of incubation periods. Collectively, these results argue that GPPrP is a better, more rapid substrate than BoPrP, HuPrP, or chimeric Mo/HuPrP expressed in Tg mice for propagating BSE and vCJD prions with high fidelity.

Several potential features of the GPPrP sequence may give rise to the enhanced BSE and vCJD prion replication kinetics observed. Unlike other mammalian PrPs, GPPrP has a deletion of 10

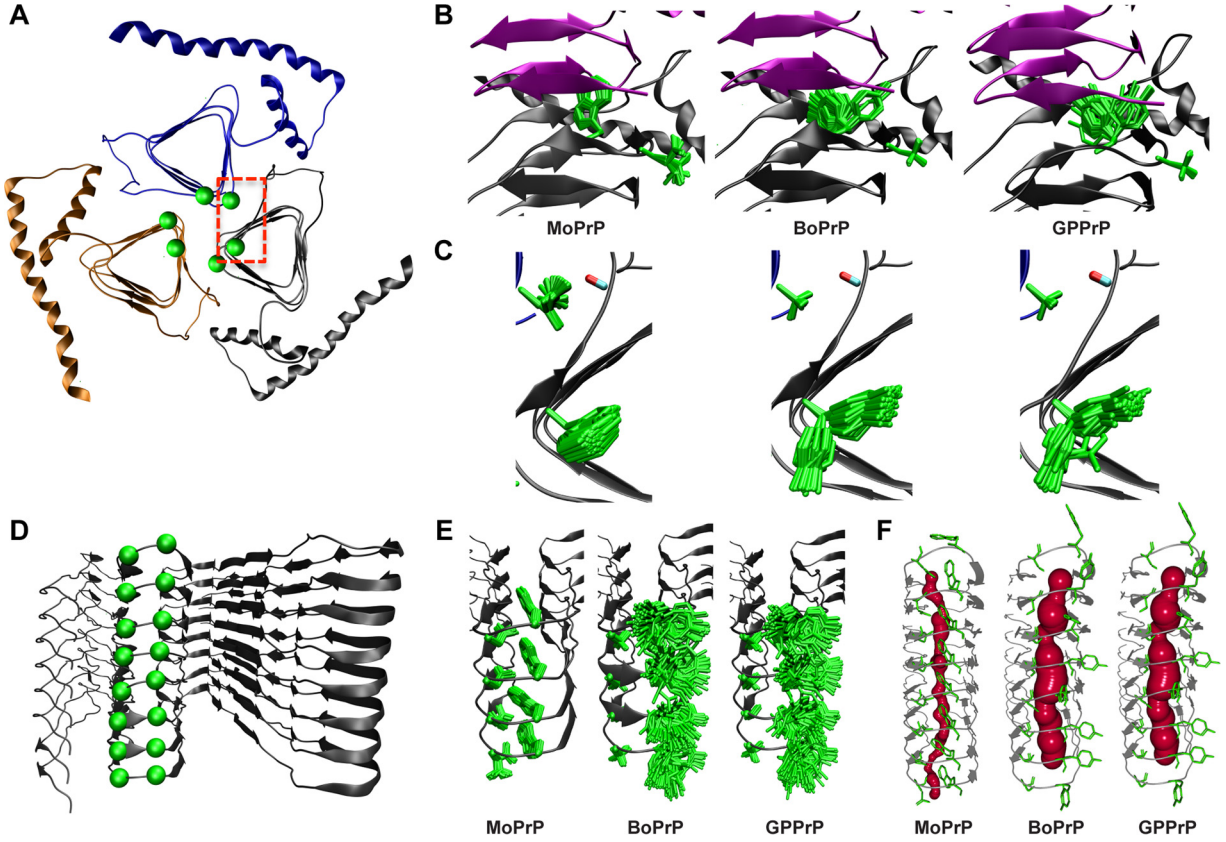

COLOR

FIG 7 Comparison of PrP^{Sc} structural models generated by using MoPrP, BoPrP, or GPPrP sequences. (A) Axial trimer of the β-helix PrP^{Sc} model (MoPrP sequence) showing the backbone positions of residues 142 (Asn) and 144 (Trp) in green. (B) Visualization of the interactions between stacked subunits (purple and gray) in the β-helix models of all three PrP sequences. Stick representations show the positions of the residue 142 and 144 side chains (green; MoPrP numbering) in all 100 generated models. (C) Closeup of the red dashed box in panel A. Highlight of the potential hydrogen bonding interaction between residue 142 (upper green side chain; Asn in MoPrP, Ser in both BoPrP and GPPrP) and the backbone carbonyl on the adjacent axial subunit (red). (D) Positions of residues 142 and 144 (green) in the PIRIBS-A model of $MoPrP^{Sc}$. (E) Visualization of the stacking interactions in the PIRIBS-A models of all three PrP sequences. Stick representations of the positions of the residue 142 and 144 side chains (green) in the 100 best-scoring models show the instability of residue 144 (right green side chain; Trp in MoPrP, Tyr in both BoPrP and GPPrP) in the GP and Bo PrP^{Sc} scaffolds. (F) Closeup of the void volume (maroon) in the three PIRIBS-A-based models showing a similar large channel in both the BoPrP and GPPrP models that is not present in the MoPrP model. Panels A to E were prepared with VMD, and panel F was prepared with CAVER Analyst.

residues that occurs N terminal to the octapeptide repeat domain (Fig. 2) (39). However, this region of PrP is thought to be dispensable for prion replication (66, 67), suggesting that the receptiveness of GPPrP for BSE and vCJD prions is likely to be encoded elsewhere in PrP. Another possibility is that the unique endoproteolytic-processing properties of GPPrP play a role. We found that GPPrP undergoes so-called "β cleavage" to produce the C2 PrP endoproteolytic fragment much more efficiently than MoPrP (Fig. 1). The PrP C2 fragment is similar in molecular weight to the PK-resistant core of PrP^{Sc}, and C2 levels increase dramatically during prion disease (68). Although Tg mice expressing a C2-like PrP allele are fully susceptible to prions, incubation periods are protracted in these mice, suggesting that the C2 fragment, if anything, delays the kinetics of prion replication (67). Thus, the increased presence of PrP C2 fragments in Tg(GPPrP) mice is unlikely to be responsible for accelerating the transmission of BSE and vCJD prions.

Structural models generated by threading the sequences of GPPrP and BoPrP onto the β-helix and PIRIBS models of $MoPrP^{Sc}$ implied that the GPPrP and BoPrP sequences are incompatible with these models. In particular, GPPrP- and BoPrP-specific amino acid residues at positions 142 and 144 are predicted to generate unfavorable structural changes in $MoPrP^{Sc}$. Interestingly, the predicted structural changes were very similar for the GPPrP and BoPrP sequences, suggesting that these two PrP sequences may be similarly capable of adopting an alternate PrP^{Sc} structure, such as the one present in the BSE and vCJD strains. This may explain why faithful transmission of BSE prions can be readily achieved in Tg(GPPrP) and Tg(BoPrP) mice, whereas the replication of mouse prions, such as the RML strain, is prevented or delayed (69). Although BSE prions are transmitted efficiently to WT and Tg(MoPrP) mice (43), serial passaging and strain characterization studies have revealed that mouse-passaged BSE prions exhibit properties vastly different from those of the original BSE strain (31, 58, 70). Therefore, the structural incompatibility conferred by MoPrP-specific residues at positions 142 and 144 may promote prion strain adaptation upon exposure to BSE prions. It is important to note that the β-helix and PIRIBS $MoPrP^{Sc}$ structures that served as templates for the $GPPrP^{Sc}$ and $BoPrP^{Sc}$ structures are themselves models with associated limitations (71). Thus, insights gained from using these models need to be confirmed experimentally.

Our finding that Tg(GPPrP) mice were susceptible to vCJD prions but not sCJD MM1, MM2, or VV2 prions is in contrast to the finding that Tg1014 mice exhibit shorter incubation periods of both vCJD and sCJD MM1 prions than mice expressing WT HuPrP (65). Interestingly, HuPrP also contains the GPPrP- and BoPrP-specific residues at positions 142 and 144. Thus, a strain barrier conferred by residue 142 and 144 variants, as opposed to a species barrier, may mediate the differential transmission of human prion strains in Tg(GPPrP) mice. These data demonstrating that vCJD and BSE prions are transmitted more rapidly to Tg(GPPrP) mice than to mice expressing HuPrP may also indicate that the HuPrP sequence has evolved to confer resistance to exogenous, as well as endogenous, prion strains (72, 73).

To the best of our knowledge, Tg23454 mice exhibit the shortest BSE and vCJD prion incubation periods described to date. Although Tg mice expressing BVPrP exhibit BVPrP-adapted vCJD and BSE prion incubation periods of ~40 and ~60 days, respectively, the incubation periods of both strains upon initial passage were >300 days (25). It may be possible to decrease the incubation periods for BSE and vCJD prions further by generating Tg mice that express chimeric Mo/GPPrP molecules, as this strategy has proven highly effective at reducing the incubation periods of sCJD MM1 prions (64, 65), or by utilizing chimeric Mo/BVPrPs. Because it has been estimated that 1 out of 2,000 individuals in the United Kingdom may possess abnormal PrP species in the appendix because of BSE exposure (74), that vCJD can be transmitted by transfusion of contaminated blood (75–77), and that prions can be amplified from the blood and urine of vCJD patients (78, 79), sensitive and rapid bioassays for BSE and vCJD prions will be critical to measuring infectivity levels in biological tissues and to assessing the risk of horizontal vCJD transmission.

ACKNOWLEDGMENTS

We thank the staff at the UCSF Hunters Point Animal Facility for their assistance with the mouse bioassays and Marta Gavidia for mouse genotyping. We also thank Robert Will and James Ironside of the National CJD Surveillance Unit (University of Edinburgh, Edinburgh, United Kingdom) for the vCJD patient brain sample and Jun Tateishi of Kyushu University (Fukuoka, Japan) for the guinea pig-passaged sCJD sample.

This work was supported by grants from the National Institutes of Health (AG021601, AG02132, and AG010770) and the Sherman Fairchild Foundation. J.C.W. was supported by a K99 grant from the National Institute on Aging (AG042453). The funders had no role in the study design, data collection, or the interpretation of experiments.

FUNDING INFORMATION

AQ: fund

This work, including the efforts of Stanley B. Prusiner, was funded by Sherman Fairchild Foundation. This work, including the efforts of Joel C. Watts, Kurt Giles, Daniel J. Saltzberg, Brittany N. Dugger, Smita Patel, Abby Oehler, Sumita Bhardwaj, Andrej Sali, and Stanley B. Prusiner, was funded by HHS | National Institutes of Health (NIH) (AG021601, AG02132, and AG010770). This work, including the efforts of Joel C. Watts, was funded by HHS | NIH | National Institute on Aging (NIA) (AG042453).

REFERENCES

1. **Prusiner SB.** 2012. A unifying role for prions in neurodegenerative diseases. Science **336:**1511–1513. http://dx.doi.org/10.1126/science.1222951.
2. **Jucker M, Walker LC.** 2013. Self-propagation of pathogenic protein aggregates in neurodegenerative diseases. Nature **501:**45–51. http://dx.doi.org/10.1038/nature12481.
3. **Prusiner SB.** 1982. Novel proteinaceous infectious particles cause scrapie. Science **216:**136–144. http://dx.doi.org/10.1126/science.6801762.
4. **Colby DW, Prusiner SB.** 2011. Prions. Cold Spring Harb Perspect Biol **3:**a006833.
5. **Will RG, Ironside JW, Zeidler M, Cousens SN, Estibeiro K, Alperovitch A, Poser S, Pocchiari M, Hofman A, Smith PG.** 1996. A new variant of Creutzfeldt-Jakob disease in the UK. Lancet **347:**921–925. http://dx.doi.org/10.1016/S0140-6736(96)91412-9.
6. **Collinge J, Sidle KCL, Meads J, Ironside J, Hill AF.** 1996. Molecular analysis of prion strain variation and the aetiology of "new variant" CJD. Nature **383:**685–690. http://dx.doi.org/10.1038/383685a0.
7. **Riek R, Hornemann S, Wider G, Billeter M, Glockshuber R, Wüthrich K.** 1996. NMR structure of the mouse prion protein domain PrP(121-231). Nature **382:**180–182. http://dx.doi.org/10.1038/382180a0.
8. **Zhang H, Stöckel J, Mehlhorn I, Groth D, Baldwin MA, Prusiner SB, James TL, Cohen FE.** 1997. Physical studies of conformational plasticity in a recombinant prion protein. Biochemistry **36:**3543–3553. http://dx.doi.org/10.1021/bi961965r.
9. **Zahn R, Liu A, Lührs T, Riek R, von Schroetter C, López García F, Billeter M, Calzolai L, Wider G, Wüthrich K.** 2000. NMR solution structure of the human prion protein. Proc Natl Acad Sci U S A **97:**145–150. http://dx.doi.org/10.1073/pnas.97.1.145.
10. **Pan K-M, Baldwin M, Nguyen J, Gasset M, Serban A, Groth D, Mehlhorn I, Huang Z, Fletterick RJ, Cohen FE, Prusiner SB.** 1993. Conversion of α-helices into β-sheets features in the formation of the scrapie prion proteins. Proc Natl Acad Sci U S A **90:**10962–10966. http://dx.doi.org/10.1073/pnas.90.23.10962.
11. **McKinley MP, Bolton DC, Prusiner SB.** 1983. A protease-resistant protein is a structural component of the scrapie prion. Cell **35:**57–62. http://dx.doi.org/10.1016/0092-8674(83)90207-6.
12. **Pattison IH, Millson GC.** 1961. Scrapie produced experimentally in goats with special reference to the clinical syndrome. J Comp Pathol **71:**101–108. http://dx.doi.org/10.1016/S0368-1742(61)80013-1.
13. **Bessen RA, Marsh RF.** 1992. Identification of two biologically distinct strains of transmissible mink encephalopathy in hamsters. J Gen Virol **73:**329–334. http://dx.doi.org/10.1099/0022-1317-73-2-329.
14. **DeArmond SJ, Sánchez H, Yehiely F, Qiu Y, Ninchak-Casey A, Daggett V, Camerino AP, Cayetano J, Rogers M, Groth D, Torchia M, Tremblay P, Scott MR, Cohen FE, Prusiner SB.** 1997. Selective neuronal targeting in prion disease. Neuron **19:**1337–1348. http://dx.doi.org/10.1016/S0896-6273(00)80424-9.
15. **Parchi P, Giese A, Capellari S, Brown P, Schulz-Schaeffer W, Windl O, Zerr I, Budka H, Kopp N, Piccardo P, Poser S, Rojiani A, Streichemberger N, Julien J, Vital C, Ghetti B, Gambetti P, Kretzschmar H.** 1999. Classification of sporadic Creutzfeldt-Jakob disease based on molecular and phenotypic analysis of 300 subjects. Ann Neurol **46:**224–233.
16. **Telling GC, Parchi P, DeArmond SJ, Cortelli P, Montagna P, Gabizon R, Mastrianni J, Lugaresi E, Gambetti P, Prusiner SB.** 1996. Evidence for the conformation of the pathologic isoform of the prion protein enciphering and propagating prion diversity. Science **274:**2079–2082. http://dx.doi.org/10.1126/science.274.5295.2079.
17. **Bessen RA, Kocisko DA, Raymond GJ, Nandan S, Lansbury PT, Caughey B.** 1995. Non-genetic propagation of strain-specific properties of scrapie prion protein. Nature **375:**698–700. http://dx.doi.org/10.1038/375698a0.
18. **Pattison IH.** 1965. Experiments with scrapie with special reference to the nature of the agent and the pathology of the disease, p 249–257. *In* Gajdusek DC, Gibbs CJ, Jr, Alpers MP (ed), Slow, latent and temperate virus infections, NINDB monograph 2. U.S. Government Printing Office, Washington, DC.
19. **Scott M, Foster D, Mirenda C, Serban D, Coufal F, Wälchli M, Torchia M, Groth D, Carlson G, DeArmond SJ, Westaway D, Prusiner SB.** 1989. Transgenic mice expressing hamster prion protein produce species-specific scrapie infectivity and amyloid plaques. Cell **59:**847–857. http://dx.doi.org/10.1016/0092-8674(89)90608-9.
20. **Peretz D, Williamson RA, Legname G, Matsunaga Y, Vergara J, Burton D, DeArmond SJ, Prusiner SB, Scott MR.** 2002. A change in the conformation of prions accompanies the emergence of a new prion strain. Neuron **34:**921–932. http://dx.doi.org/10.1016/S0896-6273(02)00726-2.
21. **Nonno R, Di Bari MA, Cardone F, Vaccari G, Fazzi P, Dell'Omo G, Cartoni C, Ingrosso L, Boyle A, Galeno R, Sbriccoli M, Lipp HP, Bruce M, Pocchiari M, Agrimi U.** 2006. Efficient transmission and character-

ization of Creutzfeldt-Jakob disease strains in bank voles. PLoS Pathog **2:**e12. http://dx.doi.org/10.1371/journal.ppat.0020012.

22. **Agrimi U, Nonno R, Dell'Omo G, Di Bari MA, Conte M, Chiappini B, Esposito E, Di Guardo G, Windl O, Vaccari G, Lipp HP.** 2008. Prion protein amino acid determinants of differential susceptibility and molecular feature of prion strains in mice and voles. PLoS Pathog **4:**e1000113. http://dx.doi.org/10.1371/journal.ppat.1000113.
23. **Di Bari MA, Nonno R, Castilla J, D'Agostino C, Pirisinu L, Riccardi G, Conte M, Richt J, Kunkle R, Langeveld J, Vaccari G, Agrimi U.** 2013. Chronic wasting disease in bank voles: characterisation of the shortest incubation time model for prion diseases. PLoS Pathog **9:**e1003219. http://dx.doi.org/10.1371/journal.ppat.1003219.
24. **Watts JC, Giles K, Stöhr J, Oehler A, Bhardwaj S, Grillo SK, Patel S, DeArmond SJ, Prusiner SB.** 2012. Spontaneous generation of rapidly transmissible prions in transgenic mice expressing wild-type bank vole prion protein. Proc Natl Acad Sci U S A **109:**3498–3503. http://dx.doi.org/10.1073/pnas.1121556109.
25. **Watts JC, Giles K, Patel S, Oehler A, DeArmond SJ, Prusiner SB.** 2014. Evidence that bank vole PrP is a universal acceptor for prions. PLoS Pathog **10:**e1003990. http://dx.doi.org/10.1371/journal.ppat.1003990.
26. **Asante EA, Linehan JM, Desbruslais M, Joiner S, Gowland I, Wood AL, Welch J, Hill AF, Lloyd SE, Wadsworth JD, Collinge J.** 2002. BSE prions propagate as either variant CJD-like or sporadic CJD-like prion strains in transgenic mice expressing human prion protein. EMBO J **21:**6358–6366. http://dx.doi.org/10.1093/emboj/cdf653.
27. **Hill AF, Desbruslais M, Joiner S, Sidle KCL, Gowland I, Collinge J, Doey LJ, Lantos P.** 1997. The same prion strain causes vCJD and BSE. Nature **389:**448–450. http://dx.doi.org/10.1038/38925.
28. **Collinge J, Palmer MS, Sidle KC, Hill AF, Gowland I, Meads J, Asante E, Bradley R, Doey LJ, Lantos PL.** 1995. Unaltered susceptibility to BSE in transgenic mice expressing human prion protein. Nature **378:**779–783. http://dx.doi.org/10.1038/378779a0.
29. **Fraser H, Bruce ME, Chree A, McConnell I, Wells GAH.** 1992. Transmission of bovine spongiform encephalopathy and scrapie to mice. J Gen Virol **73:**1891–1897. http://dx.doi.org/10.1099/0022-1317-73-8-1891.
30. **Bruce ME, Will RG, Ironside JW, McConnell I, Drummond D, Suttie A, McCardle L, Chree A, Hope J, Birkett C, Cousens S, Fraser H, Bostock CJ.** 1997. Transmissions to mice indicate that 'new variant' CJD is caused by the BSE agent. Nature **389:**498–501. http://dx.doi.org/10.1038/39057.
31. **Lasmézas CI, Deslys J-P, Robain O, Jaegly A, Beringue V, Peyrin J-M, Fournier J-G, Hauw J-J, Rossier J, Dormont D.** 1997. Transmission of the BSE agent to mice in the absence of detectable abnormal prion protein. Science **275:**402–405. http://dx.doi.org/10.1126/science.275.5298.402.
32. **Collinge J, Clarke AR.** 2007. A general model of prion strains and their pathogenicity. Science **318:**930–936. http://dx.doi.org/10.1126/science.1138718.
33. **Scott MR, Peretz D, Nguyen H-OB, DeArmond SJ, Prusiner SB.** 2005. Transmission barriers for bovine, ovine, and human prions in transgenic mice. J Virol **79:**5259–5271. http://dx.doi.org/10.1128/JVI.79.9.5259-5271.2005.
34. **Gibbs CJ, Jr, Gajdusek DC, Asher DM, Alpers MP, Beck E, Daniel PM, Matthews WB.** 1968. Creutzfeldt-Jakob disease (spongiform encephalopathy): transmission to the chimpanzee. Science **161:**388–389. http://dx.doi.org/10.1126/science.161.3839.388.
35. **Manuelidis EE.** 1975. Transmission of Creutzfeldt-Jakob disease from man to the guinea pig. Science **190:**571–572.
36. **Manuelidis E, Kim J, Angelo J, Manuelidis L.** 1976. Serial propagation of Creutzfeldt-Jakob disease in guinea pigs. Proc Natl Acad Sci U S A **73:**223–227. http://dx.doi.org/10.1073/pnas.73.1.223.
37. **Tateishi J, Sato Y, Koga M, Doi H, Ohta M.** 1980. Experimental transmission of human subacute spongiform encephalopathy to small rodents. I. Clinical and histological observations. Acta Neuropathol **51:**127–134.
38. **Tateishi J, Kitamoto T, Hoque MZ, Furukawa H.** 1996. Experimental transmission of Creutzfeldt-Jakob disease and related diseases to rodents. Neurology **46:**532–537. http://dx.doi.org/10.1212/WNL.46.2.532.
39. **Safar JG, Giles K, Lessard P, Letessier F, Patel S, Serban A, DeArmond SJ, Prusiner SB.** 2011. Conserved properties of human and bovine prion strains on transmission to guinea pigs. Lab Invest **91:**1326–1336. http://dx.doi.org/10.1038/labinvest.2011.89.
40. **Furuoka H, Horiuchi M, Yamakawa Y, Sata T.** 2011. Predominant involvement of the cerebellum in guinea pigs infected with bovine spongiform encephalopathy (BSE). J Comp Pathol **144:**269–276. http://dx.doi.org/10.1016/j.jcpa.2010.10.004.
41. **Scott MR, Köhler R, Foster D, Prusiner SB.** 1992. Chimeric prion protein expression in cultured cells and transgenic mice. Protein Sci **1:**986–997. http://dx.doi.org/10.1002/pro.5560010804.
42. **Büeler H, Fisher M, Lang Y, Bluethmann H, Lipp H-P, DeArmond SJ, Prusiner SB, Aguet M, Weissmann C.** 1992. Normal development and behaviour of mice lacking the neuronal cell-surface PrP protein. Nature **356:**577–582. http://dx.doi.org/10.1038/356577a0.
43. **Scott MR, Safar J, Telling G, Nguyen O, Groth D, Torchia M, Koehler R, Tremblay P, Walther D, Cohen FE, DeArmond SJ, Prusiner SB.** 1997. Identification of a prion protein epitope modulating transmission of bovine spongiform encephalopathy prions to transgenic mice. Proc Natl Acad Sci U S A **94:**14279–14284. http://dx.doi.org/10.1073/pnas.94.26.14279.
44. **Carlson GA, Goodman PA, Lovett M, Taylor BA, Marshall ST, Peterson-Torchia M, Westaway D, Prusiner SB.** 1988. Genetics and polymorphism of the mouse prion gene complex: control of scrapie incubation time. Mol Cell Biol **8:**5528–5540. http://dx.doi.org/10.1128/MCB.8.12.5528.
45. **Safar JG, Scott M, Monaghan J, Deering C, Didorenko S, Vergara J, Ball H, Legname G, Leclerc E, Solforosi L, Serban H, Groth D, Burton DR, Prusiner SB, Williamson RA.** 2002. Measuring prions causing bovine spongiform encephalopathy or chronic wasting disease by immunoassays and transgenic mice. Nat Biotechnol **20:**1147–1150. http://dx.doi.org/10.1038/nbt748.
46. **Kascsak RJ, Rubenstein R, Merz PA, Tonna-DeMasi M, Fersko R, Carp RI, Wisniewski HM, Diringer H.** 1987. Mouse polyclonal and monoclonal antibody to scrapie-associated fibril proteins. J Virol **61:**3688–3693.
47. **Sievers F, Wilm A, Dineen D, Gibson TJ, Karplus K, Li W, Lopez R, McWilliam H, Remmert M, Söding J, Thompson JD, Higgins DG.** 2011. Fast, scalable generation of high-quality protein multiple sequence alignments using Clustal Omega. Mol Syst Biol **7:**539.
48. **Sali A, Blundell TL.** 1993. Comparative protein modelling by satisfaction of spatial restraints. J Mol Biol **234:**779–815. http://dx.doi.org/10.1006/jmbi.1993.1626.
49. **Govaerts C, Wille H, Prusiner SB, Cohen FE.** 2004. Evidence for assembly of prions with left-handed β-helices into trimers. Proc Natl Acad Sci U S A **101:**8342–8347. http://dx.doi.org/10.1073/pnas.0402254101.
50. **Groveman BR, Dolan MA, Taubner LM, Kraus A, Wickner RB, Caughey B.** 2014. Parallel in-register intermolecular β-sheet architectures for prion-seeded prion protein (PrP) amyloids. J Biol Chem **289:**24129–24142. http://dx.doi.org/10.1074/jbc.M114.578344.
51. **Baker EN, Hubbard RE.** 1984. Hydrogen bonding in globular proteins. Prog Biophys Mol Biol **44:**97–179. http://dx.doi.org/10.1016/0079-6107(84)90007-5.
52. **Humphrey W, Dalke A, Schulten K.** 1996. VMD: visual molecular dynamics. J Mol Graph **14:**33–38. http://dx.doi.org/10.1016/0263-7855(96)00018-5.
53. **Kozlikova B, Sebestova E, Sustr V, Brezovsky J, Strnad O, Daniel L, Bednar D, Pavelka A, Manak M, Bezdeka M, Benes P, Kotry M, Gora A, Damborsky J, Sochor J.** 2014. CAVER Analyst 1.0: graphic tool for interactive visualization and analysis of tunnels and channels in protein structures. Bioinformatics **30:**2684–2685. http://dx.doi.org/10.1093/bioinformatics/btu364.
54. **Premzl M, Gamulin V.** 2007. Comparative genomic analysis of prion genes. BMC Genomics **8:**1–14. http://dx.doi.org/10.1186/1471-2164-8-1.
55. **Altmeppen HC, Puig B, Dohler F, Thurm DK, Falker C, Krasemann S, Glatzel M.** 2012. Proteolytic processing of the prion protein in health and disease. Am J Neurodegener Dis **1:**15–31.
56. **Oliveira-Martins JB, Yusa S-I, Calella AM, Bridel C, Baumann F, Dametto P, Aguzzi A.** 2010. Unexpected tolerance of α-cleavage of the prion protein to sequence variations. PLoS One **5:**e9107. http://dx.doi.org/10.1371/journal.pone.0009107.
57. **Gibbs CJ, Jr, Gajdusek DC.** 1973. Experimental subacute spongiform virus encephalopathies in primates and other laboratory animals. Science **182:**67–68. http://dx.doi.org/10.1126/science.182.4107.67.
58. **Scott MR, Will R, Ironside J, Nguyen H-OB, Tremblay P, DeArmond SJ, Prusiner SB.** 1999. Compelling transgenetic evidence for transmission of bovine spongiform encephalopathy prions to humans. Proc Natl Acad Sci U S A **96:**15137–15142. http://dx.doi.org/10.1073/pnas.96.26.15137.
59. **Telling GC, Scott M, Mastrianni J, Gabizon R, Torchia M, Cohen FE, DeArmond SJ, Prusiner SB.** 1995. Prion propagation in mice expressing human and chimeric PrP transgenes implicates the interaction of cellular

PrP with another protein. Cell **83:**79–90. http://dx.doi.org/10.1016/0092-8674(95)90236-8.

60. **Deleault NR, Piro JR, Walsh DJ, Wang F, Ma J, Geoghegan JC, Supattapone S.** 2012. Isolation of phosphatidylethanolamine as a solitary cofactor for prion formation in the absence of nucleic acids. Proc Natl Acad Sci U S A **109:**8546–8551. http://dx.doi.org/10.1073/pnas.1204498109.
61. **Tamgüney G, Francis KP, Giles K, Lemus A, DeArmond SJ, Prusiner SB.** 2009. Measuring prions by bioluminescence imaging. Proc Natl Acad Sci U S A **106:**15002–15006. http://dx.doi.org/10.1073/pnas.0907339106.
62. **Watts JC, Prusiner SB.** 2014. Mouse models for studying the formation and propagation of prions. J Biol Chem **289:**19841–19849. http://dx.doi.org/10.1074/jbc.R114.550707.
63. **Buschmann A, Pfaff E, Reifenberg K, Müller HM, Groschup MH.** 2000. Detection of cattle-derived BSE prions using transgenic mice overexpressing bovine PrP^{C}. Arch Virol Suppl **16:**75–86.
64. **Korth C, Kaneko K, Groth D, Heye N, Telling G, Mastrianni J, Parchi P, Gambetti P, Will R, Ironside J, Heinrich C, Tremblay P, DeArmond SJ, Prusiner SB.** 2003. Abbreviated incubation times for human prions in mice expressing a chimeric mouse-human prion protein transgene. Proc Natl Acad Sci U S A **100:**4784–4789. http://dx.doi.org/10.1073/pnas.2627989100.
65. **Giles K, Glidden DV, Patel S, Korth C, Groth D, Lemus A, DeArmond SJ, Prusiner SB.** 2010. Human prion strain selection in transgenic mice. Ann Neurol **68:**151–161. http://dx.doi.org/10.1002/ana.22104.
66. **Fischer M, Rülicke T, Raeber A, Sailer A, Moser M, Oesch B, Brandner S, Aguzzi A, Weissmann C.** 1996. Prion protein (PrP) with amino-proximal deletions restoring susceptibility of PrP knockout mice to scrapie. EMBO J **15:**1255–1264.
67. **Supattapone S, Muramoto T, Legname G, Mehlhorn I, Cohen FE, DeArmond SJ, Prusiner SB, Scott MR.** 2001. Identification of two prion protein regions that modify scrapie incubation time. J Virol **75:**1408–1413. http://dx.doi.org/10.1128/JVI.75.3.1408-1413.2001.
68. **Chen SG, Teplow DB, Parchi P, Teller JK, Gambetti P, Autilio-Gambetti L.** 1995. Truncated forms of the human prion protein in normal brain and in prion diseases. J Biol Chem **270:**19173–19180. http://dx.doi.org/10.1074/jbc.270.32.19173.
69. **Torres J-M, Espinosa J-C, Aguilar-Calvo P, Herva M-E, Relaño-Ginés A, Villa-Diaz A, Morales M, Parra B, Alamillo E, Brun A, Castilla J, Molina S, Hawkins SAC, Andreoletti O.** 2014. Elements modulating the prion species barrier and its passage consequences. PLoS One **9:**e89722. http://dx.doi.org/10.1371/journal.pone.0089722.
70. **Giles K, Glidden DV, Beckwith R, Seoanes R, Peretz D, DeArmond SJ, Prusiner SB.** 2008. Resistance of bovine spongiform encephalopathy (BSE) prions to inactivation. PLoS Pathog **4:**e1000206. http://dx.doi.org/10.1371/journal.ppat.1000206.
71. **Requena JR, Wille H.** 2014. The structure of the infectious prion protein: experimental data and molecular models. Prion **8:**60–66. http://dx.doi.org/10.4161/pri.28368.
72. **Mead S, Stumpf MP, Whitfield J, Beck JA, Poulter M, Campbell T, Uphill JB, Goldstein D, Alpers M, Fisher EM, Collinge J.** 2003. Balancing selection at the prion protein gene consistent with prehistoric kurulike epidemics. Science **300:**640–643. http://dx.doi.org/10.1126/science.1083320.
73. **Asante EA, Smidak M, Grimshaw A, Houghton R, Tomlinson A, Jeelani A, Jakubcova T, Hamdan S, Richard-Londt A, Linehan JM, Brandner S, Alpers M, Whitfield J, Mead S, Wadsworth JDF, Collinge J.** 2015. A naturally occurring variant of the human prion protein completely prevents prion disease. Nature **522:**478–481. http://dx.doi.org/10.1038/nature14510.
74. **Gill ON, Spencer Y, Richard-Loendt A, Kelly C, Dabaghian R, Boyes L, Linehan J, Simmons M, Webb P, Bellerby P, Andrews N, Hilton DA, Ironside JW, Beck J, Poulter M, Mead S, Brandner S.** 2013. Prevalent abnormal prion protein in human appendixes after bovine spongiform encephalopathy epizootic: large scale survey. BMJ **347:**f5675. http://dx.doi.org/10.1136/bmj.f5675.
75. **Llewelyn CA, Hewitt PE, Knight RS, Amar K, Cousens S, Mackenzie J, Will RG.** 2004. Possible transmission of variant Creutzfeldt-Jakob disease by blood transfusion. Lancet **363:**417–421. http://dx.doi.org/10.1016/S0140-6736(04)15486-X.
76. **Peden AH, Head MW, Ritchie DL, Bell JE, Ironside JW.** 2004. Preclinical vCJD after blood transfusion in a *PRNP* codon 129 heterozygous patient. Lancet **364:**527–529. http://dx.doi.org/10.1016/S0140-6736(04)16811-6.
77. **Wroe SJ, Pal S, Siddique D, Hyare H, Macfarlane R, Joiner S, Linehan JM, Brandner S, Wadsworth JD, Hewitt P, Collinge J.** 2006. Clinical presentation and pre-mortem diagnosis of variant Creutzfeldt-Jakob disease associated with blood transfusion: a case report. Lancet **368:**2061–2067. http://dx.doi.org/10.1016/S0140-6736(06)69835-8.
78. **Moda F, Gambetti P, Notari S, Concha-Marambio L, Catania M, Park K-W, Maderna E, Suardi S, Haïk S, Brandel J-P, Ironside J, Knight R, Tagliavini F, Soto C.** 2014. Prions in the urine of patients with variant Creutzfeldt-Jakob disease. N Engl J Med **371:**530–539. http://dx.doi.org/10.1056/NEJMoa1404401.
79. **Lacroux C, Comoy E, Moudjou M, Perret-Liaudet A, Lugan S, Litaise C, Simmons H, Jas-Duval C, Lantier I, Béringue V, Groschup M, Fichet G, Costes P, Streichenberger N, Lantier F, Deslys JP, Vilette D, Andréoletti O.** 2014. Preclinical detection of variant CJD and BSE prions in blood. PLoS Pathog **10:**e1004202. http://dx.doi.org/10.1371/journal.ppat.1004202.

JOBNAME: AUTHOR QUERIES PAGE: 1 SESS: 5 OUTPUT: Fri Jul 22 20:28:42 2016
/rich4/zjv-jvi/zjv-jvi/zjv01916/zjv1962d16z

AUTHOR QUERIES

AUTHOR PLEASE ANSWER ALL QUERIES 1

AQau—Please confirm the given-names and surnames are identified properly by the colors. ■= Given-Name, ■= Surname

AQaff—Please confirm the following full affiliations or correct here as necessary. This is what will appear in the online HTML version:

[a]Institute for Neurodegenerative Diseases, University of California, San Francisco, San Francisco, California, USA
[b]California Institute for Quantitative Biosciences (QB3), University of California, San Francisco, San Francisco, California, USA
[c]Department of Neurology, University of California, San Francisco, San Francisco, California, USA
[d]Department of Biochemistry and Biophysics, University of California, San Francisco, San Francisco, California, USA
[e]Department of Bioengineering and Therapeutic Sciences, University of California, San Francisco, San Francisco, California, USA
[f]Department of Pharmaceutical Chemistry, University of California, San Francisco, San Francisco, California, USA

AQaff—This affiliation line will appear in the PDF version of the article and matches that on page 1 of the proof; corrections to this affiliation line may be made here **or** on page 1 of the proof:

Institute for Neurodegenerative Diseases,[a] California Institute for Quantitative Biosciences (QB3),[b] and Departments of Neurology,[c] Biochemistry and Biophysics,[d] Bioengineering and Therapeutic Sciences,[e] and Pharmaceutical Chemistry, University of California, San Francisco, San Francisco, California, USA[f]

AQfund—The Funding Information section includes information that you provided on the submission form when you submitted the manuscript. Any specific funding source(s) that you identified, along with its associated author(s) and, if applicable, grant number(s), appears in a paragraph (each funder-grant-author combination identified has a dedicated sentence). Any funding statement that you provided on the submission form appears in a separate paragraph. Please check the Funding Information section for accuracy, since the information may be restyled by ASM staff during preparation of the proofs. The final style of presentation is at the discretion of ASM staff.

Funder	Grant(s)	Author(s)
Sherman Fairchild Foundation		Stanley B. Prusiner
HHS | National Institutes of Health (NIH)	AG021601, AG02132, AG010770	Joel C. Watts, Kurt Giles, Daniel J. Saltzberg, Brittany N. Dugger, Smita Patel, Abby Oehler, Sumita Bhardwaj, Andrej Sali, Stanley B. Prusiner

AUTHOR QUERIES

AUTHOR PLEASE ANSWER ALL QUERIES 2

HHS | NIH | National Institute on Aging (NIA)	AG042453	Joel C. Watts

AQA—Au/?Change to "2-(*N*-morpholino)ethanesulfonic acid" OK? If not, spell out "MES."

AQB—Au/?Change from "polyvinylidene fluoride" to "polyvinylidene difluoride" OK?

AQC—Au/ASM policy requires that sequence/protein/microarray data be available to the public upon online posting of the article, so please verify the accuracy of accession numbers for such data (particularly for new sequences) and that each number retrieves the full record of the data when used in a search in the database (not just the home page). If the link takes you to an empty record, instruct the production staff to remove the link. Please also verify the database link, if included (hotlinks can be added only to GenBank, PDB, DDBJ, GEO, ArrayExpress, and BioSample/BioProject accession numbers). If the accession number is for a database that cannot be linked, please add the database name to the text. If the accession numbers for new data are not publicly accessible by the proof stage, publication of your article may be delayed; please contact the ASM production editor immediately with the expected release date.

AQD—Ed: Link "a" is missing in Table No.2 body. Please check—Ptr.